

Identification of nuclear fragmentation isotopes in FOOT

B. SPADAVECCHIA ON BEHALF OF THE FOOT COLLABORATION

Università di Torino, Dipartimento di Fisica - Torino, Italy & INFN, Sezione di Torino, Italy

Summary. — The mass of beam fragments produced by ^{12}C at 200 MeV/u, impinging on a 5-mm thick graphite target, was measured by using the FOOT experiment electronic setup. This is the first time such a result was obtained, by combining measurements from three scintillating detectors: the TOF-Wall (TW) and Start Counter (SC), used for Z identification and Time-Of-Flight (TOF) measurement, and the BGO calorimeter (CALO) which stops the fragments, thus providing kinetic energy (E_{kin}) measurements.

In spite of the preliminary nature of these results, isotopes with Z from 1 to 6 were identified, in some cases already providing mass measurements within the required 5% experimental resolution for A.

1. – Introduction

The FOOT (FragmentatiOn Of Target) experiment aims at measuring nuclear fragmentation cross sections for processes of interest in Charged Particle Therapy (CPT) and Radioprotection in Space (RPS). The nuclei involved range from ^1H to ^{56}Fe , with energies within 50-400 MeV/u in the first case, up to 1 GeV/u in the second case.

Both beam and target particles can produce highly relevant secondaries. In CPT, projectile fragmentation within human tissues (and tissue fragmentation itself) might reduce the dose delivery precision of cancer radiotherapy treatments [1]; radiation hazards, falling in the RPS case, are also one of the major risks for space exploration beyond Low Earth Orbit (LEO) [2]. In order to address such problems, it is necessary to benchmark and update the existing Monte Carlo (MC) nuclear models, by measuring differential (dE/dE_{kin}) and double differential cross sections ($d^2E/(d\Omega \cdot dE_{kin})$) with a precision of 5% and 10% respectively.

Double differential cross sections are currently available only for ^{12}C at few energy values [3]: filling this gap with the aforementioned precision requires a resolution in charge (Z) and mass (A) identification of 2-3% and 5% respectively [4].

2. – Experimental setup

The FOOT experiment aims at filling the aforementioned gap via several combinations of beams (He, C, O) and targets (C, C_2H_4 , PMMA).

In this study, ^{12}C at 200 MeV/u was used as the primary beam in a data taking session that took place at CNAO (Centro Nazionale di Adroterapia Oncologica) in Pavia, Italy.

The setup in use, shown in Fig. 1, has an angular acceptance of $\approx 6^\circ$ and is therefore optimized for detecting fragments with $Z > 2$. It includes, along the beam direction:

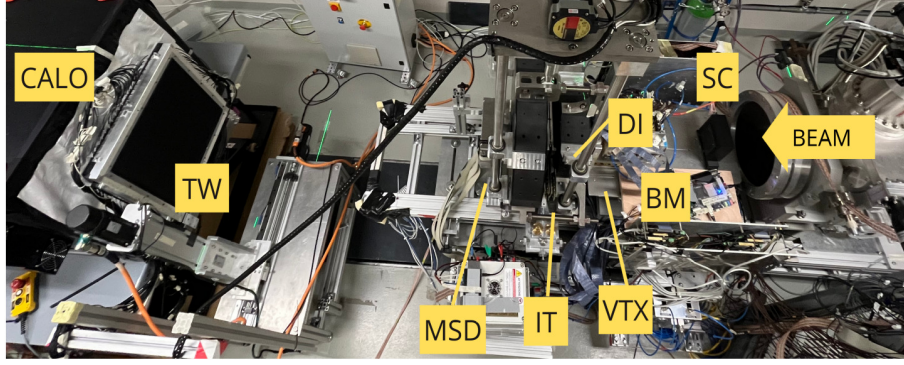


Fig. 1. – Experimental setup used during the CNAO 2024 data taking, with the electronic spectrometer for fragments identification.

- the Start Counter (SC) - a $250\ \mu\text{m}$ thick EJ-228 scintillator layer, which measures the incoming ion flux and is the main event trigger (time resolution $\sigma_t \sim 10 - 100$ ps depending on the beam species/energy) [4];
- the Beam Monitor (BM) - a drift chamber for beam profile reconstruction along the x and y direction, filled with a 80/20% gas mixture of Ar and CO_2 , with a space resolution of $60 - 100\ \mu\text{m}$ and a 90% efficiency [5];
- the target - a 5-mm thick graphite layer;
- the Vertex detector (VTX) - 4 MIMOSA28 (M28) monolithic pixel sensors, close to the target in order to reconstruct fragmentation vertices;
- two permanent magnets (DI), in Halbach configuration, deflecting fragments with an approximately dipolar magnetic field;
- the Inner Tracking (ITR) station - two planes of M28 pixel sensors in order to track fragments inside the magnetic field;
- Microstrip Silicon Detectors (MSD) - three x-y planes, each consisting of two perpendicular Single-Sided Silicon Detector (SSSD) sensors, to track fragments downstream the magnetic region and provide redundant measurements of dE/dx ;
- the TOF-Wall (TW) - 40 bars of EJ-200 plastic scintillator arranged in two, 3-mm thick, orthogonal layers providing direct dE/dx measurements for Z identification and TOF measurements in combination with the SC;
- the Calorimeter (CALO) - consisting of 320 BGO crystals each coupled to a Silicon PhotoMultiplier (SiPM), it is designed to stop the fragments and measure their kinetic energy E_{kin} .

The beam rate was kept below 1 kHz, in order to avoid pile up effects in the VTX, the detector with the slowest readout response ($\approx 200\ \mu\text{s}$).

3. – CALO calibration

The CALO was operationally divided into 4 quarters and irradiated with proton (p) and Carbon (C) ions for a series of calibration runs, by shifting the beam via the CNAO scanning magnets in a so-called "sweeping mode" (Fig. 2).

For the two ion species, 4 energy points were taken at energies between 100-175 MeV and 115-330 MeV/u respectively. Each crystal has a slightly different response curve with respect to energy (E) and atomic number (Z), owing to:

- pile-up effects for optical photons impinging on the SiPM-based readout system, whose reset time is $\approx 7 - 10$ ns;
- reduction of the signal amplitude with increasing particle range [6];
- quenching effects, leading to a reduction of the scintillation signal per unit length (dS/dx) with respect to the stopping power (dE/dx) [7].

For each crystal and ion species, the ADC peak values were corrected in temperature [6] and their dependence on E was modeled with the following Modified Birks Function (MBF):

$$(1) \quad ADC(E) = \frac{p_0 E^2}{1 + p_1 E + p_2 E^2}.$$

4. – CALO resolution

For Carbon points, a resolution close to 2% was found; a sub-optimal resolution ($\approx 3\%$) was achieved on proton points; however, it must be recalled that this experimental setup is not optimized for such fragments. The achieved resolution σ_E for p at 100, 125 and 150 MeV and C at 115 and 200 MeV/u was reported in Fig. 3 and was fitted with the well known function

$$(2) \quad \sigma_E/E = \sqrt{S/E + N/E^2 + C},$$

modeling the intrinsic fluctuations in the energy release process (S), the electronics-driven noise (N) and calibration uncertainties (C) [8].

At higher energies, charge sharing phenomena among neighbor crystals occur with higher probability and are not completely under control: for this reason, the last p point and the last two C energy points were not used in the fit.

In a previous campaign, carried out in Heidelberg in 2022 with p, He, C and O ions, it was observed that each of the 3 MBF parameters p_i can be modeled with a power-law function with respect to Z. The three parameters are normalized to their values for Carbon $p_i(C)$, since the same ion species was used in previous calibration campaigns under different work conditions:

$$(3) \quad \frac{p_i}{p_i(C)} = a_{0i} Z^{a_{1i}}, \text{ where } i = 1, 2, 3.$$

Eventually, 301/320 crystals were successfully calibrated: to each of them are associated 6 power-law parameters and 3 MBF parameters from Carbon, thus allowing Z-dependent energy reconstruction.

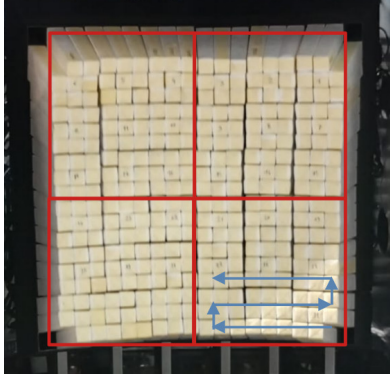


Fig. 2. – CALO frontal view, with a schematic representation of the beam scanning carried out under "sweeping mode".

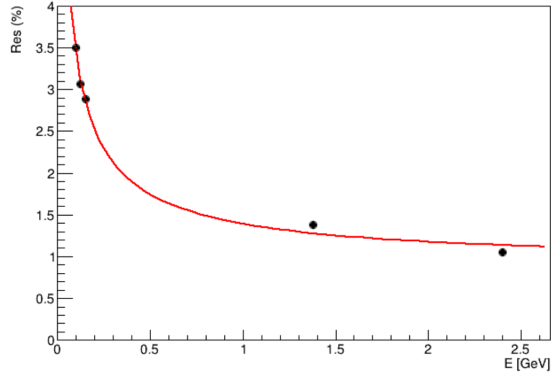


Fig. 3. – Resolution values plotted with respect to energy, with the fit function reported in Eq. 2. The first three points were taken with protons, the last two ones with C ions.

5. – Mass reconstruction in fragmentation events

Incoming fragments on the Calorimeter generate cluster signals: as shown in Eq. 3, in order to properly reconstruct their energy, the TW detector must provide Z identification.

Active TW bars from the two X-Y layers are structured in TW points, whose atomic number is assigned through dE/dx measurements with known reconstruction efficiency [9]. The TW also provides time measurements t_f in coincidence with the SC, which provides the acquisition starting time t_0 ; therefore, the Time-Of-Flight (TOF) of fragments is obtained as

$$(4) \quad TOF = t_f - t_0 - t_i,$$

where t_i is the time in which primaries reach the target and can be easily estimated from their known energy.

Among all CALO cluster - TW point combinations, only the ones having minimum distance are preserved, thus assigning to each fragment a charge (Z) and Time-Of-Flight (TOF). The latter is used to compute the Lorentz factor β ; since the tracking system (in particular IT and MSD detectors) is not available for analysis yet, β was computed under uniform velocity approximation:

$$(5) \quad \beta = L/TOF,$$

where L is the distance between the target center and the assigned TW point, thus neglecting any deflection induced by the magnetic field.

From β , $\gamma = (1 - \beta^2)^{-1/2}$ can be computed, in order to obtain the fragment mass:

$$(6) \quad A = \frac{E_{kin}[MeV] \cdot u}{0.931494 MeV \cdot (\gamma - 1)}.$$

In terms of isotopic abundance, quite all the expected stable or long-life isotopes (~ 100 ms - 1 s) are visible in experimental data, though with a clear sub-optimal resolution.

In addition to this, there is a clear underestimation of the reconstructed mass values with respect to the nominal ones. This effect becomes relevant for high Z values and is due to a systematic overestimation of β : indeed, the uniform velocity approximation neglects the fragment energy loss across the tracking system. Finally, some artifacts due to reasons being investigated are present: in the specific case of ^{12}C , the small peak on the left is related to a single crystal response instability (most likely caused by a mechanical trauma), while the peak on the right is possibly due to multiple fragments being included in the same CALO cluster.

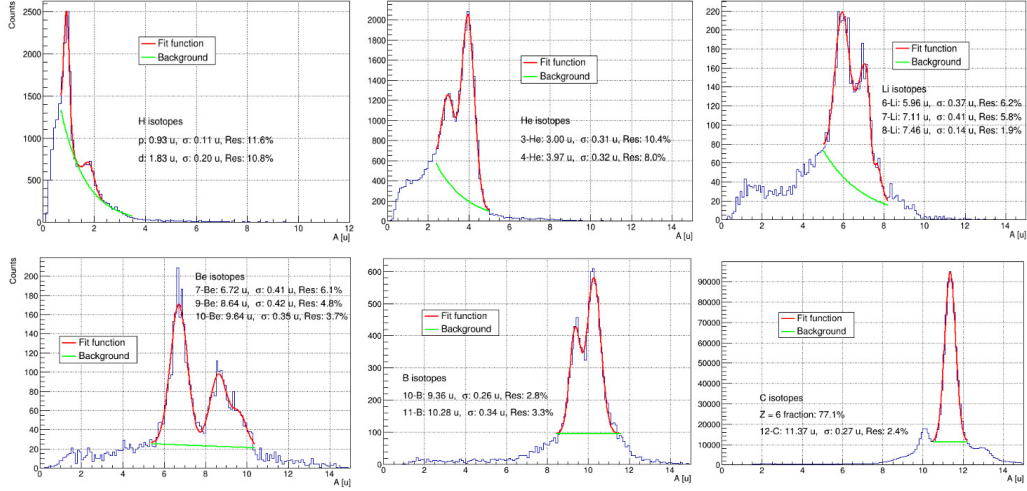


Fig. 4. – Gaussian fit of data-reconstructed mass peaks, expected from MC simulation. A decreasing exponential was used as a background modeling function.

Fig. 4 reports the fit of all successfully identified mass peaks from $Z = 1$ to $Z = 6$, each modeled by a Gaussian curve combined with an overall decreasing exponential function: indeed, out-of-target fragmentation must be taken into account.

Peak values and their widths (σ) are reported in Fig. 5, showing that the A underestimation (mostly due to the Lorentz factor overestimation) with respect to nominal mass values can be modeled by a first-order polynomial and is approximately of 5%.

Fig. 6 reports the resolution values for the peaks considered in Fig. 5. A resolution better than 5% was achieved for ^{10}Be , ^{10}B , ^{11}B and ^{12}C , while for smaller A (and Z) values there is a clear worsening with respect to the goal resolution: the most likely, but not exclusive cause is energy calibration with respect to Z (for $Z = [2, 5]$).

6. – Conclusion

For the first time, the FOOT experiment has measured mass distributions for ion species produced in fragmentation events, in particular for ^{12}C interactions at 200 MeV/u with a 5-mm thick graphite target. The results are very preliminary but promising, since almost all the foreseen isotopes from $Z = 1$ to $Z = 6$ were successfully reconstructed.

Mass reconstruction is affected by systematic errors due to uniform velocity approximation and multiple fragments clustering, which the tracking system might help reduce. Isotope abundance was quite well modeled, although the 5% goal resolution was reliably

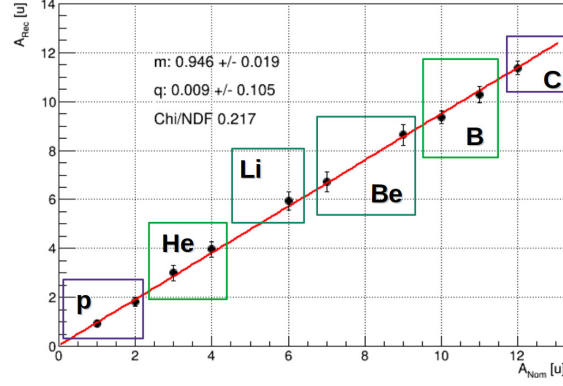


Fig. 5. – Reconstructed mass peak values (A_{rec} [u]) plotted against their nominal values (A_{nom} [u]), and fitted with a first order polynomial.

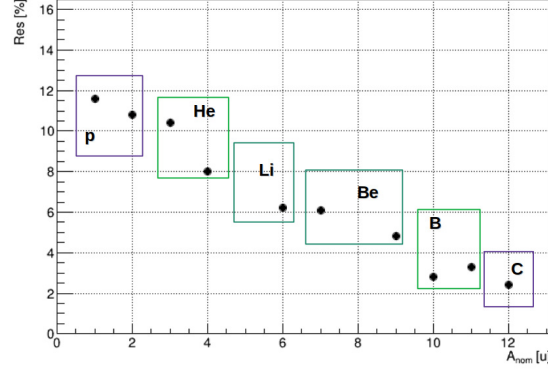


Fig. 6. – Mass peak resolution values [%] with respect to A_{nom} [u], compared with MC reconstructed peak resolution (in red).

achieved only for the highest A values. For this reason, all sources of statistical and experimental errors must be investigated, while the CALO calibration in energy and Z requires further optimization.

REFERENCES

- [1] TOMASSINO F. ET AL., *International Journal of Particle Therapy*, **2015** (2)
- [2] HEINBOCKEL J.H. ET AL., *Advances in Space Research*, **2011** (47)
- [3] DUDOUET J. ET AL., *Physical Review C*, **2013** (88)
- [4] TOPPI M. ET AL., *Frontiers in Physics*, **2021** (8)
- [5] DONG Y. ET AL., *Nucl Instrum Methods Phys Res, Sec A*, **2021** (986)
- [6] BARTOSIK N. ET AL., *Journal of Instrumentation*, **2025** (20)
- [7] BIRKS J.B., in *The Theory and Practice of Scintillation Counting*, edited by D.R. HILLMAN & SONS (Pergamon Press, Oxford) 1964, p. 187.
- [8] FABJAN C.W. AND GIANOTTI F., *Reviews of Modern Physics*, **2003** (75)
- [9] TOPPI M., SARTI A., ALEXANDROV A. ET AL., *Frontiers in Physics*, **2022** (10)